Non-linear electro-elastic coupling in non-centrosymmetric materials

Jacky Even, Laurent Pedesseau, Chahira Hajlaoui, Claudine Katan, Jean-Marc Jancu

Non-linear electro-elastic coupling in non-centrosymmetric materials

2012 J. Phys.: Conf. Ser. 367 012005

(http://iopscience.iop.org/1742-6596/367/1/012005)

Journal of Physics: Conference Series **367** (2012) 012005 doi:10.1088/1742-6596/367/1/012005

Non-linear electro-elastic coupling in non-centrosymmetric materials

J Even[1], L Pedesseau[1], C Hajlaoui[1], C Katan[1,2] and J-M Jancu[1]
[1] Université Européenne de Bretagne, INSA, FOTON, UMR 6082, F-35708 Rennes, France
[2] CNRS, Institut des Sciences Chimiques de Rennes, UMR 6226, 35042 Rennes, France

E-mail: jacky.even@insa-rennes.fr

Abstract. We propose an extended symmetry-based thermodynamical model of third-order electro-elastic coupling. The entanglement of electrostriction non-linear piezoelectricity and other non-linear phenomena, is studied in details at the same level of theory. Symmetry properties of materials and nanostructures are taken into account. Density Functional Theory (DFT) is used to calculate the complete set of linear and non-linear coefficients. Electrostriction dominates for nitride compounds in the Würtzite structure, but non-linear elasticity and piezoelectricity must be taken into account for strain and electric field evaluation.

1. Introduction

A complete model of third-order electro-elastic coupling has recently been proposed [1]. It is an extension of a previous thermodynamical approach [2] (quoted as ATK model in this paper). The latter seems to be almost ignored up to now, although a number of misinterpretation or errors could have been avoided recently in the literature. In this work, the ATK model is combined systematically with symmetry analyses and DFT calculations to evaluate consistently the various linear and non-linear coefficients, especially in non centrosymmetric materials. Symmetry properties of third-order elastic constants are well known [3], but have been extensively studied for third-order coupled constants only more recently [4]. In this paper, third-order coefficients are mostly determined from finite difference studies of material's polarisation or stress tensor under various electrical or strain conditions. We show in section 2. that the non-linear tensors can be strongly entangled. Actually, in the same theoretical model, coefficients defined for a specific thermodynamical potential should not be mixed with others without caution. Experimental determination of piezoelectric and electrostrictive entangled components must also rely on careful definitions of experimental conditions which makes such measurements very tedious and tricky [5]. The direction of the applied field and the frequency behaviour are useful tools to separate the strains which are arising from piezoelectricity and electrostriction.

2. Thermodynamic potentials and derivatives

2.1. Thermodynamic potentials and first order derivatives

Thermodynamic potentials are introduced using standard definitions for the free energy and enthalpy, $F = U - TS$ and $G = U - \sigma_i \eta_i - TS$, and the transformed free energy and enthalpy

$F_e = U - TS - E_l D_l$ and $G_e = U - \sigma_i \eta_i - TS - E_l D_l$. The D_l, E_l vectors and the η_i, σ_i strain-stress tensors (in Voigt notation) are associated respectively to the l,m,n,u,v,o and i,j,k,p,q,r indices varying between 1-3 and 1-6 respectively.
The first order derivatives of the thermodynamic potentials are:

- $dG = -SdT - \eta_i d\sigma_i + E_l dD_l$
- $dG_e = -SdT - \eta_i d\sigma_i - D_l dE_l$
- $dF_e = -SdT + \sigma_i d\eta_i - D_l dE_l$
- $dF = -SdT + \sigma_i d\eta_i + E_l dD_l$

In the following, most expressions are related to F_e, G and G_e.

2.2. Second order derivatives

Three second-order derivatives in relation to D_l, E_l, η_i and σ_i are defined for each of the thermodynamic potentials.

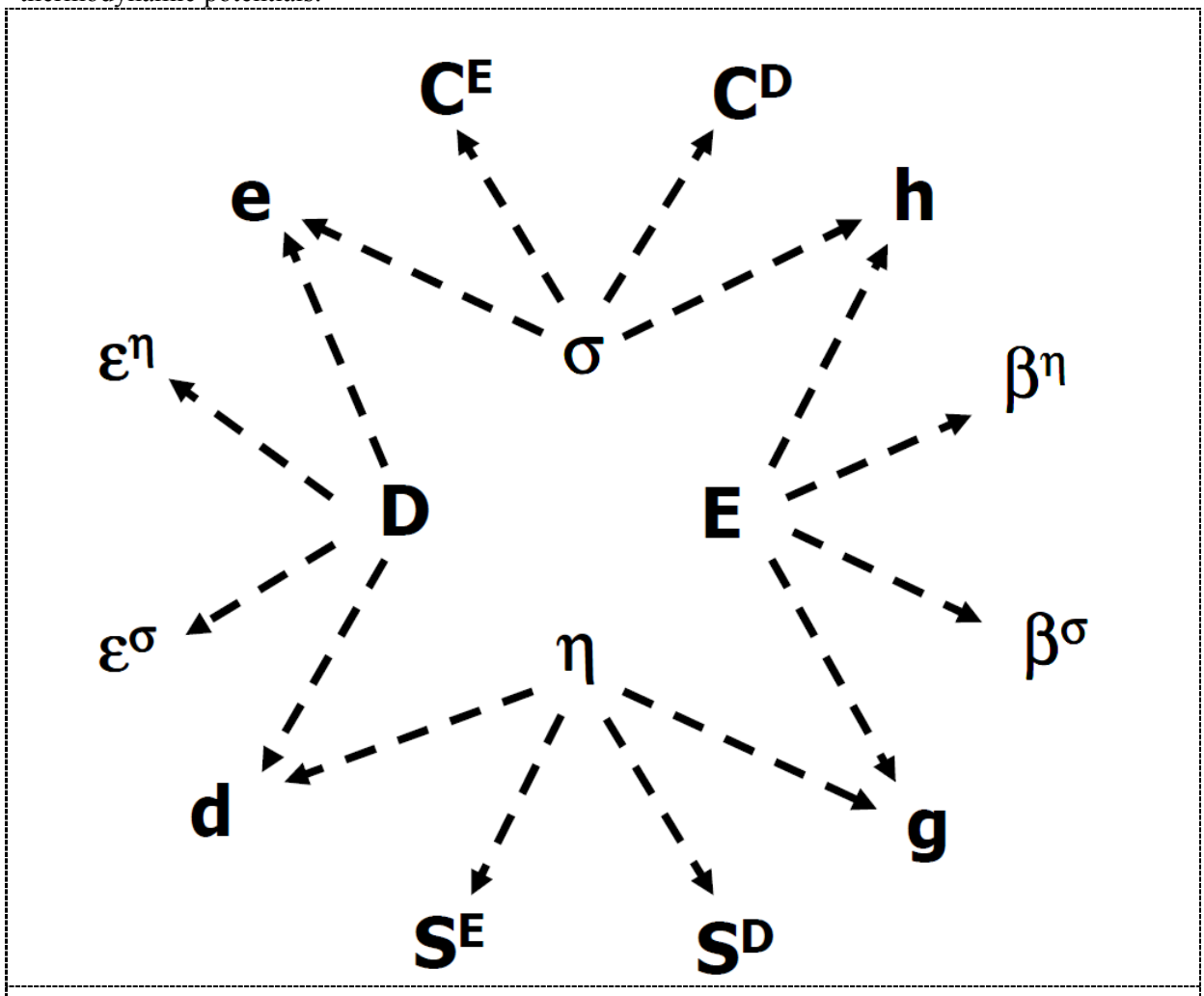

Figure 1. Schematic representation of the relations between thermodynamic variables (inner variables) and second order derivatives of the thermodynamic potentials (outer variables). For clarity, minus signs are not shown.

Figure 1 is a schematic representation of the relations between thermodynamic variables and second order derivatives of the thermodynamic potentials (for the clarity of the figure minus signs are not shown) :

- $d\sigma_i = C^E{}_{ij} d\eta_j - e_{il} dE_l$ and $dD_l = e_{li} d\eta_i + \varepsilon^\eta{}_{lm} dE_m$ for F_e
- $d\eta_i = S^E{}_{ij} d\sigma_j + d_{il} dE_l$ and $dD_l = d_{li} d\sigma_i + \varepsilon^\sigma{}_{lm} dE_m$ for G_e
- $d\eta_i = S^D{}_{ij} d\sigma_j + g_{il} dD_l$ and $dE_l = -g_{li} d\sigma_i + \beta^\sigma{}_{lm} dD_m$ for G

The second-order derivatives of the thermodynamic potentials are related to each other by exact expressions:

- $\varepsilon^\sigma{}_{lm} - \varepsilon^\eta{}_{lm} = e_{lj} S^E{}_{ji} e_{im}$
- $e_{il} = C^E{}_{ij} d_{jl}$
- $S^E{}_{ij} - S^D{}_{ij} = g_{il} d_{lj}$

2.3. Third order derivatives

Four third-order derivatives are defined for each of the thermodynamic potentials. Figure 2 is a schematic representation of the relations between thermodynamic variables and third order derivatives of the thermodynamic potentials (minus signs are not shown). Some of these derivatives are common to different thermodynamic variables, for example :

- $B_{lij} = \left.\frac{\partial e_{li}}{\partial \eta_j}\right|_{E,T} = B_{ijl} = -\left.\frac{\partial C_{ij}}{\partial E_l}\right|_{\eta,T} = -\left|\frac{\partial^2 \sigma_i}{\partial \eta_j \partial E_l}\right| = \left.\frac{\partial^2 D_l}{\partial \eta_i \partial \eta_j}\right|_{E,T} = -\left|\frac{\partial^3 F_e}{\partial \eta_i \partial \eta_j \partial E_l}\right|$

The third order derivatives are also connected to second order derivatives :

- $dC^E{}_{ij} = C^E{}_{ijk} d\eta_k - B_{ijl} dE_l$, $de_{li} = B_{lij} d\eta_j + L_{\lim} dE_m$ and $d\varepsilon^\eta{}_{lm} = L_{lmi} d\eta_i + \varepsilon^\eta{}_{lmn} dE_n$
- $dS^E{}_{ij} = S^E{}_{ijk} d\sigma_k + F_{ijl} dE_l$, $dd_{li} = F_{lij} d\sigma_j + M_{\lim} dE_m$ and $d\varepsilon^\sigma{}_{lm} = M_{lmi} d\sigma_i + \varepsilon^\sigma{}_{lmn} dE_n$
- $dS^D{}_{ij} = S^D{}_{ijk} d\sigma_k + R_{ijl} dD_l$, $dg_{li} = R_{lij} d\sigma_j + Q_{lmi} dD_m$ and $d\beta^\sigma{}_{lm} = -Q_{lmi} d\sigma_i + \beta^\sigma{}_{lmn} dD_n$

Most of these quantities are already used in various papers [5-7], but we will focus on the non-linear piezoelectric tensors B_{lij}, F_{lij} , R_{lij} and the electrostrictive tensors L_{lmi}, M_{lmi} and Q_{lmi}. The third-order derivatives of the thermodynamic potentials are also related to each other by various exact expressions:

- $F_{lij} = S^E{}_{ik} B_{lkp} S^E{}_{pj} + e_{lk} S^E{}_{kij}$
- $R_{lij} = \beta^\sigma{}_{lm} F_{mij} - \beta^\sigma{}_{lm} \beta^\sigma{}_{nv} (M_{mni} d_{vj} + M_{mnj} d_{vi}) - \beta^\sigma{}_{lmn} d_{mi} d_{nj}$
- $Q_{lmi} = \beta^\sigma{}_{lmn} d_{ni} + \beta^\sigma{}_{mn} \beta^\sigma{}_{lv} M_{vni}$
- $M_{lmi} = (B_{lkp} d_{mp} + B_{mkp} d_{lp}) S^E{}_{ki} + L_{lmj} S^E{}_{ji} + e_{lk} e_{mj} S^E{}_{kji}$.

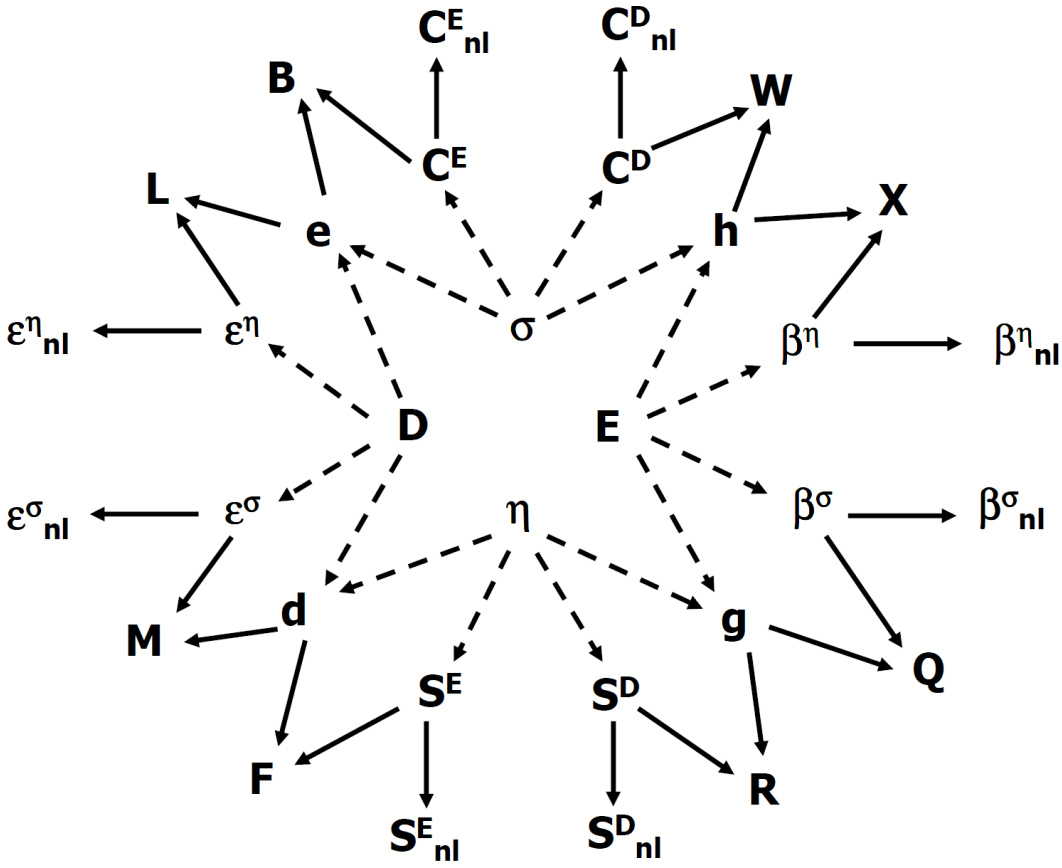

Figure 2. Schematic representation of the relations between thermodynamic variables, second derivatives and third order derivatives (outer variables) of the thermodynamic potentials. For clarity, minus signs are not shown.

3. Symmetry analysis

It has been shown in section 2. that the non-linear tensors can be strongly entangled. For instance, in the case of non-centrosymmetric materials, an additional term related to the linear piezoelectricity and the non-linear susceptibility must be added to the commonly used relation $Q_{lmi} = \beta^{\sigma}{}_{mn}\beta^{\sigma}{}_{lv}M_{vni}$ [5]. It is necessary to use symmetry properties of the materials in order to check whether or not the entanglement has to be taken into account. In order to get a first insight into the influence of lattice symmetry, we may compare materials which crystallise in a cubic lattice associated either to the m3m (e.g. diamond or undistorted perovskite lattices) and 432 point groups. In both cases, the linear piezoelectric tensors and non-linear susceptibilities are vanishing: $e_{li} = d_{li} = g_{li} = 0$ and $\varepsilon^{\eta}{}_{lmn} = \varepsilon^{\sigma}{}_{lmn} = \beta^{\sigma}{}_{lmn} = 0$. Only six independent non-linear elastic constants and compliances exist: $C^{E}{}_{ijk}$, $S^{E}{}_{ijk} = S^{D}{}_{ijk}$. Q_{lmi}, M_{lmi} and L_{lmi} tensors related to electrostriction are simply connected, like in isotropic materials: $Q_{lmi} = \beta^{\sigma}{}_{mn}\beta^{\sigma}{}_{lv}M_{vni}$ and $M_{lmi} = L_{lmj}S^{E}{}_{ji}$, although the number of independent coefficients is larger. The only difference between the m3m and 432 point groups comes from the non-linear piezoelectricity phenomenon which appears only in the 432 case. Among the thirty-two crystal classes, eleven are centrosymmetric (m3m case) and twenty-one are non-centrosymmetric, but of these, 432 is a special case. For point group 432, non-linear piezoelectricity

and electrostriction, are indeed disentangled. The various non-linear piezoelectric tensors are simply connected and only one independent component B_{124} has to be determined: $F_{124} = (S_{11}^E - S_{12}^E)B_{124}S_{44}^E = \varepsilon^\sigma R_{124}$. Ten of the non-centrosymmetric crystal classes represent the polar crystal classes, which show a spontaneous polarization. For all this crystal classes, the entanglement of non linear piezoelectricity, non linear dielectric susceptibility and electrostriction is very strong. The hexagonal 6mm polar crystal class corresponds to a number of important materials in the wurtzite structure. The tensors describing non-linear piezoelectricity have 8 independent components : B_{311}, B_{312}, B_{313}, B_{333}, B_{344}, B_{115}, B_{125}, B_{135} whereas the tensor describing electrostriction has 6 components : L_{11}, L_{12}, L_{13}, L_{31}, L_{33}, L_{44}. Using relation $M_{lmi} = (B_{lkp}d_{mp} + B_{mkp}d_{lp})S^E{}_{ki} + L_{lmj}S^E{}_{ji} + e_{lk}e_{mj}S^E{}_{kji}$, we can compare the non-linear piezoelectric, electrostrictive and elastic contributions. In the case of nitride compounds like GaN, the electrostrictive contribution is the most important, but non-linear piezoelectric effect can not be ignored [1].

4. Determination of non-linear coefficients using density functional theory

The methods of density-functional perturbation theory (DFPT) may be used to calculate various physical responses. In fact the efficient use of the "2n+1" theorem [8], using only by-products of a first-order perturbation calculation, in principle gives the second and third-order derivatives of the total energy at the level of the ATK model, if the atomic-displacement variables are eliminated. Second-order derivatives may be used with an existing DFPT implementation [9] to calculate various physical response properties of insulating crystals, including elastic constants, linear piezoelectric tensors, linear dielectric susceptibility, as well as tensor properties related to internal atomic displacements like Born charges. Third-order derivatives of the total energy are related to a number of physical properties described in this work, like the non-linear electrical susceptibility, the non-linear elasticity, the photo-elastic and electrostrictive effects. However, most practical implementations of the DFPT are restricted to some quantities related to internal atomic displacements. DFT simulations are performed using a state of the art DFT implementation [9] within the local density approximation (LDA). Plane wave basis sets were used with a kinetic energy cutoff of 950 eV after convergence studies. The sets of k-points were generated following the procedure of Pack and Monkhorst and Pack [10] namely 10 10 10. Polarisation and stress tensor components can be studied as a function of the electric field and strain tensor components. We applied various electrical or strain conditions for the DFT determination of all the coefficients in the case of the GaN and AlN crystals [1]. In figure 3, the variations of σ_3 and P_3 are reported as a function of η_3 for AlN.

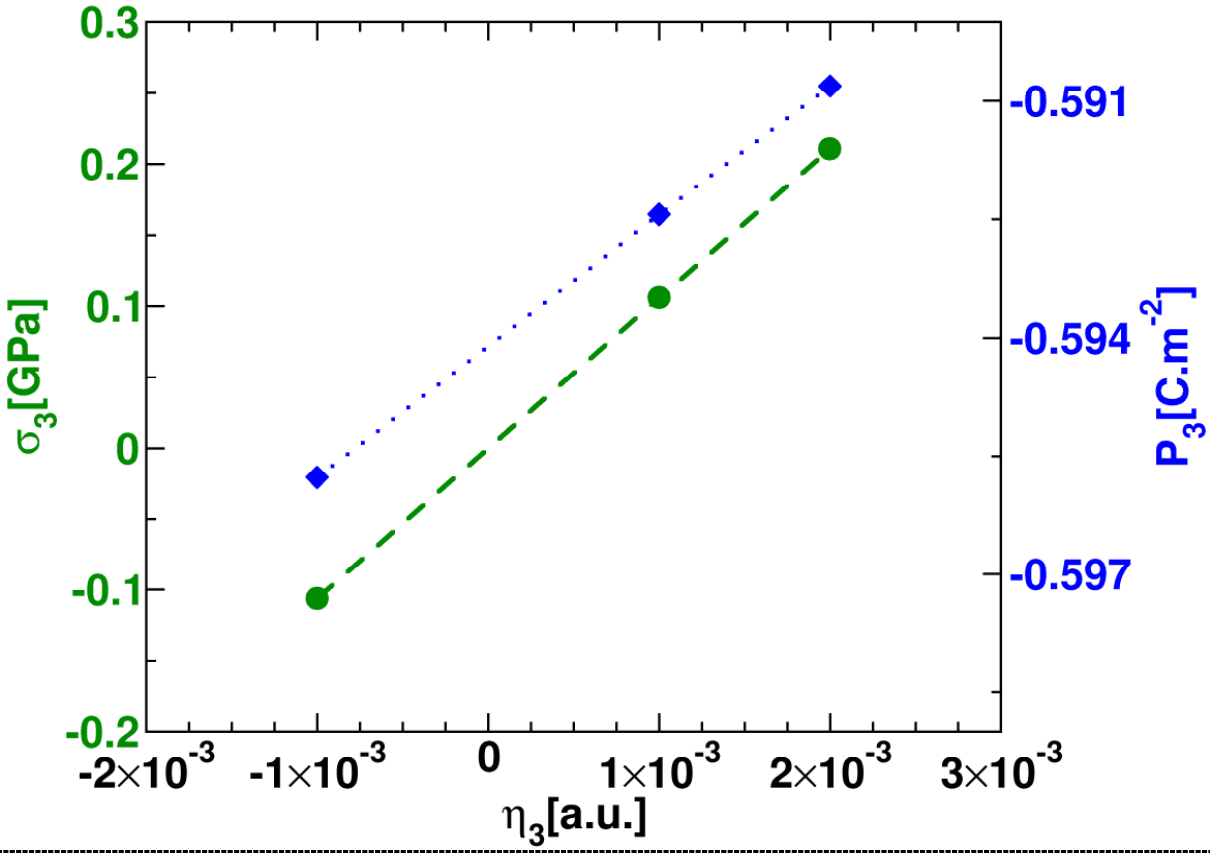

Figure 3. Variations of σ_3 and P_3 calculated using a state of the art DFT implementation [9] are reported as a function of η_3 for AlN.

Acknowledgement.
This work was performed using HPC resources from GENCI-CINES (Grant 2010-[c2010096472]) and French ANR Project INSCOOP (no ANR-11-NANO-012)

References

[1] Pedesseau L, Katan C and Even J 2012 *Appl. Phys. Lett.* **100** 031903
[2] Adam W, Tichy J and Kittinger E 1988 *J. Appl. Phys.* **84** 2556
[3] Brugger K 1965 *J. Appl. Phys.* **36** 759
[4] Grimmer H 2007 *Acta Cryst* **A63** 441
[5] Newnham R E, Sundar V, Yimnirun R, Su J and Zhang Q M 1997 *J. Phys. Chem.* **B101** 10141
[6] Bester G, Wu X, Vanderbilt D and Zunger A 2006 *Phys. Rev. Lett.* **96** 187602
[7] Gerlich D and Breazeale M A 1990 *J. Appl. Phys.* **68** 5119
[8] Hamann D R, Wu X, Rabe K M and Vanderbilt D 2005 *Phys. Rev.* **B71** 035117
[9] Gonze X, Amadon B, Anglade P M, Beuken J M, Bottin F, Boulanger P, Bruneval F, Caliste D, Caracas R, Cote M, Deutsch T, Genovese L, Ghosez Ph, Giantomassi M, Goedecker S, Hamann D R, Hermet P, Jollet F, Jomard G, Leroux S, Mancini M, Mazevet S, Oliveira M J T, Onida G, Pouillon Y, Rangel T, Rignanese G M, Sangalli D, Shaltaf R, Torrent M, Verstraete M J, Zerah G, Zwanziger J W, 2009 *Computer Phys. Commun.* **180** 2582
[10] Monkhorst H J and Pack J D, 1976 *Phys. Rev.* **B13**, 5188